SUPPLEMENTAL DATA

Patients and PET/CT Images Acquisition

In the framework of a prospective study supported by an EC FP7 grant, a PET/CT was performed in almost all patients referred to our department of Cardiovascular Surgery with a known AAA diagnosed by ultra-sound examination. Biopsies were collected in 18 patients (10 PET0 and 8 PET+) during elective surgery performed 1-4 weeks after the PET/CT examination. PET/CT data were acquired in 2 hospitals, using either a Gemini BB (16-slice CT, Philips) in 12 patients (CHU) and a Discovery LS (16-slice CT, GE Healthcare) in 6 patients (CHC). All patients fasted for at least 6 hours. Plasma blood glucose level was measured before administration of the tracer and was within normal limits in all cases. FDG (3.7 MBq/kg body weight) was injected through an indwelling catheter. The uptake time was 60 minutes. A low-dose CT (thickness 5mm, increment 5mm, voltage 120 kV, current 25 mA/slice) was first acquired, followed by the PET emission scan from the skull to the upper thighs (1-3 minutes per bed position depending on the scanner and patient's body habitus). The study was completed by an arterial phase CT (thickness 2 mm, increment 1 mm, 120 keV, 100 mA/slice). Data were corrected for decay, scatter, random, attenuation and reconstructed using an interactive 3D algorithm. Low-dose CT data were used for attenuation correction. The acquisition protocol was slightly different at the CHC: Continuous arterial phase CT from the skull to the upper thighs was performed (thickness 2.5mm, 120kVp, automatic adaptation of the amperage at each tube rotation optimized with indications provided by the scout view) and followed by the PET emission scan covering the same regions (4 minutes per bed position). Data were corrected for decay, scatter, random, attenuation and reconstructed by mean of ordered subset expectation maximization (OSEM) reconstruction algorithm performed with 2 iterations and 21 ordered subsets. CT raw data were used for attenuation correction. The standardized uptake value (SUV) was measured. As the SUVs may vary depending on the PET/CT device and protocol, we elected to express the results as AAA/liver activity ratios (rSUV), each patient acting as his own control. No difference between the mean SUV ratio was observed between the two hospitals (CHU and CHC).

Tissue Collection

The positive FDG uptake sites were localized by the surgeon (NS, who has a strong and long-standing experiment in AAA repair) by using a combination of anatomical landmarks (distance to renal artery, inferior mesenteric artery and iliac bifurcation) and measurements on pictures of PET/CT displayed on a screen in the operating room. The area of interest was further mapped in degrees relative to the anterior midline (ie, the largest sagittal diameter) of the infrarenal aorta for later intraoperative identification by the surgeon. A representative example was illustrated in Supplemental Figure 1.

Tissue Histology and Immunohistochemistry

Two 5 μm sections were performed at 100 μm distance in paraformaldehyde fixed full-thickness aortic wall and were stained with hematoxylin-eosin. Except for the α-smooth muscle actin (α-SMA) and Ki67 staining, all immunostainings were performed in an auto-stainer Ventana (Roche Molecular Biochemicals). Briefly, antigen retrieval was achieved with citrate/EDTA buffer and the different primary antibodies were incubated for 32 min. The revelation was performed with a specific kit for the Ventana (Ultra-View Universal kit, Roche). For the α-SMA staining, the antigen retrieval was achieved with 2.5% trypsin solution (Gibco, Invitrogen) and the primary antibody was added for two hours. For KI67 staining, the antigen retrieval was achieved with citrate/EDTA buffer and the antibody was added for two hours. The revelation was performed with the AEC substrate (DakoCytomation) or with the 3,3'-diaminobenzidine (DAB, DakoCytomation). The different antibodies used were α-SMA antibody (A2547, 1/300, Sigma Aldrich), KI67 (M7240, 1/100, DakoCytomation), CD-45 antibody (Ab-2, 1/100, NeoMarkers, Thermo Scientific), CD3 antibody (DakoCytomation, polyclonal, 1/300), CD20 antibody (DakoCytomation, L-20, 1/800), CD68 antibody (DakoCytomation, KP-1, 1/1800) and CD138 antibody (MCA681H, 1/100, AbD Serotec).

For CD68 and CD138 staining, the number of positive cells was counted in 10 high power fields (400× magnification). For CD45, CD3 and CD20, the number of high power fields (400× magnification) full of positive cells per square centimeter was determined. The Ki67 labeling was quantified by counting the number of positive cells in 10 fields at high magnification (×400). The

overall inflammatory infiltrate and the α-SMA labeling were evaluated by computer-assisted image analysis after image acquisition using a fully automated digital microscopy system dotSlide (Olympus) coupled with a high-resolution digital colour camera (Olympus, XC10) and the ImageJ software. The results were expressed in arbitrary units (AU) per unit surface.

Transcriptomic Analysis

Tissue samples were ground in liquid nitrogen (Dismembrator apparatus, B.Braun Biotech International). Total RNA was extracted with Trizol (TriPur, Bio-Rad) or the RiboPure™ kit (Ambion) according to the manufacturer's instructions. Total RNA was quantified with a NanoDrop (Isogen Life Sciences) and its quality assessed by Experion Automated Electrophoresis System (Bio-Rad). Only the RNA samples with a RQI >7 were used in the study. Gene expression was analysed by either semi-quantitative RT-PCR or by Real-time PCR.

The RT-PCR reactions were performed in an automated thermocycler (GeneAmp PCR system 9600) using a GeneAmp Thermostable rTth Reverse Transcriptase RNA PCR kit (Applied Biosystem) using the oligonucleotides detailed in Supplemental Table 2. For most of the tested genes, the efficiency of the RT and the PCR was controlled by adding in each reaction tube a synthetic RNA co-transcribed and co-amplified in non-competitive conditions with the same primers as the endogenous RNA but yielding an amplification product of slightly different size as previously described [1]. Briefly, 10 ng of total RNA and a known copy number of the standard synthetic RNA were reverse transcribed (70°C for 15 min). The RNA-DNA heteroduplexes were denatured for 2 min at 95°C and amplification was carried out at 94°C for 15 s, 66°C for 20 s and 72°C for 10 s. The RT-PCR products were quantified after electrophoresis on a 10% polyacrylamide gel and staining (Gelstar, Lonza) using a Fluor-S™ Multi Imager (Bio-Rad). The reaction was normalized using GAPDH as reference.

For the real-time PCR, 500 ng of total RNA was reversed transcribed using SuperScript II Reverse Transcriptase (Invitrogen). Real-Time PCR was performed in a final volume of 20 µl containing cDNA corresponding to 1 ng for mRNA, 2 µM of each primer (Supplemental Table 2) and 10 µl of the qPCR MasterMix Plus for SYBR-Green (Eurogentec) in the Abi Prism 7000 Sequence Detection

system (Applied Biosystems). The efficiency of the reaction was calculated and each reaction was normalized by the geometrical mean of GAPDH and beta-2 microglobulin.

MMP-2 and MMP-9 Zymography

Liquid nitrogen powdered tissue was extracted in 0.01M Tris, 1M NaCl and 2M urea, pH 7.5 overnight at 4°C. After centrifugation at 16000g for 10 min at 4°C, the supernatant was collected and the proteins content was quantified by a colorimetric method (Micro BSA protein assay kit, Pierce) to standardize protein loading. Samples were incubated for 1 hour at room temperature with an equal volume of denaturing buffer (0.04M Tris, 4% SDS, 20% sucrose and blue bromophenol) and loaded on a SDS-PAGE gel containing 1% of gelatin. After migration, gels were washed two times in 2% Triton-X100 at room temperature and incubated at 37° C overnight in 0.05M Tris HCl pH 7.6, 10mM $CaCl_2$. Gels were stained with Coomassie Blue, the gelatinase bands appearing as white on a blue background. For samples containing large amount of gelatinolytic activity, zymography was repeated with diluted tissue extracts to remain in the linear part of the reaction and allow a more precise calculation.

Statistical Analyses

Statistical analysis was performed by Mann-Whitney U test, and the distribution of each variable was characterized by the median and the interquartile range (IQR). For paired analysis, a Wilcoxon signed rank test was performed. Results were considered to be significant at the 5% critical level ($p < 0.05$). Correlations between inflammatory cells density and SUV were established using the Spearman's rank test for non-parametric values.

REFERENCES

1. Lambert CA, Colige AC, Munaut C, Lapiere CM, Nusgens BV. Distinct pathways in the over-expression of matrix metalloproteinases in human fibroblasts by relaxation of mechanical tension. *Matrix Biol*. 2001;20:397-408

Supplemental Table 1. Clinical features of patients presenting a positive or no FDG uptake in aneurysmal wall and applied analytical techniques.

Patient ID	Deciding factor	AAA Size (mm)	Histology and α-SMA and Ki67 labeling	Immuno labelling	Transcriptomic analysis	Zymography
No FDG uptake						
1	≥ 55 mm	67	X		na	X
2	≥ 55 mm	70	X		na	X
3	≥ 55 mm	60	X		X	X
4	≥ 55 mm	55†	X		X	X
5	≥ 55 mm	57†	X		X	X
6	Growth	54§	X		na	X
7	≥ 55 mm	80†	X		X	X
8	≥ 55 mm	56	X		X	X
9	Anxiety	53	X		X	X
10	≥ 55 mm	71	X		na	X
Positive FDG uptake						
11	Anxiety	52	X		X	X
12	Growth	54	X	X	X	X
13	Pain	40†	X	X	X	X
14	Growth	55	X	X	X	X
15	≥ 55 mm	69	X	X	na	
16	≥ 55 mm	67	X	X	X	X
17	Anxiety	57	X	X	X	
18*	Growth	53	X		na	X

* Diffuse uptake. †: neoplasia. §: renal insufficiency. na, RNA not available.

Supplemental Table 2. Oligonucleotides sequences and characteristics of amplification products.

RNA		Oligonucleotides (5'-3')	Product size	RT-PCR	RealTime PCR
GAPDH	Fwd	CCT GGC CAA GGT CAT CCA TGA CA	183	X	X
	Rev	GGG ATG ACC TTG CCC ACA GCC TT			
B2M	Fwd	GAG TAT GCC GCC GTG TG	110		X
	Rev	AAT CCA AAT GCG GCA TCT			
MMP-1	Fwd	AAA GGC CAG TAT GCA CAG CTT TC	195		X
	Rev	TTC AAC CAC TGG GCC ACT ATT TC			
MMP-2	Fwd	AGA TCT TCT TCT TCA AGG ACC GGT T	225	X	
	Rev	GGC TGG TCA GTG GCT TGG GGT A			
MMP-3	Fwd	ATG AGG TAC GAG CTG GAT ACC CAA	222	X	
	Rev	ATC AAT CTT TGA GTC AAT CCC TGG AA			
MMP-9	Fwd	GCG GAG ATT GGG AAC CAG CTG TA	208	X	
	Rev	GAC GCG CCT GTG TAC ACC CAC A			
MMP-12	Fwd	AGG AAT CGG GCC TAA AAT TG	124		X
	Rev	TGC TTT TCA GTG TTT TGG TGA			
MMP-13	Fwd	ATT AAG GAG CAT GGC GAC TTC T	171		X
	Rev	GCC GAA CTC ATG CGC AGC AA			
MMP-14	Fwd	GAG GAA GGA TGG CAA ATT CG	66		X
	Rev	AGG GAC GCC TCA TCA AAC AC			
MMP-15	Fwd	CTT GCA GAG ATG CAG CGC TTC TAC	153		X
	Rev	CTG GAT GCT AAA GGT CAG ATG GTG			
TIMP-1	Fwd	CAT CCT GTT GTT GCT GTG GCT GAT	176		X
	Rev	GTC ATC TTG ATC TCA TAA CGC TGG			
TIMP-2	Fwd	CTC GCT GGA CGT TGG AGG AAA GAA	161		X

	Rev	AGC CCA TCT GGT ACC TGT GGT TCA			
TIMP-3	Fwd	CTT CTG CAA CTC CGA CAT CGT GAT	216	X	
	Rev	CAG CAG GTA CTG GTA CTT GTT GAC			
PAI-1	Fwd	AGG GCT TCA TGC CCC ZCT TCT TCA	197	X	
	Rev	AGT AGA GGG CAT TCA CCA GCA CCA			
uPA	Fwd	ACT ACT ACG GCT CTG AAG TCA CCA	205		X
	Rev	GAA GTG TGA GAC TCT CGT GTA GAC			
RECK	Fwd	CTG TGA ACT GGC TAT TGC CTT GGA	218		X
	Rev	GGA CCA GGA GAA GAG TCT GTT CGA			
EMMPRIN	Fwd	TGA AGT CGT CAG AAC ACA TCA ACG	205		X
	Rev	GCC TCC ATG TTC AGG TTC TCA ATG			
MCP-1	Fwd	TAG CAG CCA CCT TCA TTC CCC AAG	170		X
	Rev	AAT GGT CTT GAA GAT CAC AGC TTC			
IL-1 β	Fwd	AAA CAG ATG AAG TGC TCC TTC CAG	391	X	
	Rev	TGG AGA ACA CCA CTT GTT GCT CCA			
IL-6	Fwd	AAC AAA TTC GGT ACA TCC TCG ACG	191		X
	Rev	GAT GAT TTT CAC CAG GCA AGT CTC			
IL-8	Fwd	GCC AAG GAG TGC TAA AGA ACT TAG	222		X
	Rev	GAA TTC TCA GCC CTC TTC AAA AAC			
COX-2	Fwd	TTC TCC TTG AAA GGA CTT ATG GGT AA	282		X
	Rev	AGA ACT TGC ATT GAT GGT GAC TGT TT			
TSP-1	Fwd	GTG ATG ATG ACG ATG ACA ATG ATA AA	265		X
	Rev	ATA TCA GTG TCT CTC TGG TCC ACA			
TNF-α	Fwd	CCT CTT CTC CTT CCT GAT CGT	144		X
	Rev	CGA GAA GAT GAT CTG ACT GCC			
COL1A1	Fwd	CCC ACC AAT CAC CTG CGT ACA GA	214		X
	Rev	TTC TTG GTC GGT GGG TGA CTC TGA			

Elastin	Fwd	CCG CTA AGG CAG CCA AGT ATG GA	275		X
	Rev	AGC TCC AAC CCC GTA AGT AGG AAT			
HIF-1 α	Fwd	CCC AGA TTC AGG ATC AGA CAC CTA	338		X
	Rev	CTG CTG GAA TAC TGT AAC TGT GCT T			
CD31	Fwd	GAA GGT GAT AGC CCC GGT GGA TGA	183	X	
	Rev	GCC TGG GTG GCA TTT GAG GTC ATT			
VEGF A	Fwd	CCT GGT GGA CAT CTT CCA GGA GTA		X	
	Rev	CTC ACC GCC TCG GCT TGT CAC A			
α-SMA	Fwd	GGC ATT GCC GAC CGA ATG CAG AA	236		X
	Rev	CTA GAG ACA GAG AGG AGC AGG AAA			
TGF β-1	Fwd	GGA GAG GGC CCA GCA TCT GCA A	215		X
	Rev	TGT ACT GCG TGT CCA GGC TCC AA			

Supplemental Table 3. Relative expression of selected genes in the media of AAA wall from PET0 and PET+ patients at the negative and positive site

Gene	PET0	PET+	
	(n=4)	Negative site (n=6)	Positive site (n=6)
Matrix remodeling			
MMP-1	1 (0.7-1.3)	0.6 (0.4-1.6)	1.1 (0.9-2.9)†
MMP-2	1 (0.8-1.4)	1.1 (0.8-1.1)	1.5 (1.4-1.5)
MMP-3	nd	nd	nd
MMP-9	1 (0.7-1.2)	1.2 (1.0-1.2)	0.9 (0.7-1.1)
MMP-12	1 (0.8-1.1)	0.3 (0.2-0.3)*	0.5 (0.3-1.0)†
MMP-13	1 (0.5-1.7)	0.7 (0.4-1.1)	2.7 (0.8-5.6)†
MMP-14	1 (0.9-1.2)	1.0 (0.9-1.5)	1.4 (1.3-1.5)
MMP-15	1 (0.9-1.2)	0.4 (0.4-0.7)*	1.0 (0.5-1.2)
TIMP-1	1 (0.9-1.1)	1.1 (0.8-1.3)	2.0 (1.5-2.1)**†
TIMP-2	1 (0.9-1.1)	0.6 (0.5-0.7)*	0.4 (0.4-0.5)**†
TIMP-3	1 (0.8-1.2)	0.7 (0.5-0.8)	0.7 (0.6-1.1)
PAI-1	1 (0.8-1.2)	1.0 (0.9-1.2)	1.3 (1.0-1.8)
uPA	1 (1.0-1.1)	0.9 (0.6-1.0)	1.2 (1.0-1.3)
RECK	1 (0.9-1.3)	0.5 (0.5-0.7)**	0.5 (0.3-0.7)**
EMMPRIN	1 (0.9-1.2)	0.8 (0.8-0.8)**	0.7 (0.6-0.7)**†
Structural proteins			
COL1A1	1 (0.9-1.3)	0.8 (0.7-0.9)*	1.8 (1.0-3.2)†
Elastin	1 (0.6-1.3)	0.9 (0.5-1.4)	0.3 (0.2-0.5)†
Inflammatory mediators			
MCP-1	1(0.8-1.3)	1.7 (1.1- 1.9)	1.2 (0.8-1.5)
IL-1 β	1 (0.9-1.1)	0.7 (0.6-1.0)	0.7 (0.5-1.0)
IL-6	1 (0.8-1.2)	0.9 (0.1-2.0)	2.9 (0.5-6.3)

IL-8	1 (0.6-1.3)	0.3 (0.2-0.3)*	0.3 (0.3-0.6)
COX-2	1 (0.8-1.3)	1.9 (0.7-3.9)	2.4 (1.4-2.5)
TNF-α	1 (0.9-1.6)	0.9 (0.7-1.0)	0.5 (0.5-0.5)*
TGF-β_1	1 (0.9-1.1)	0.7 (0.6-0.8)	0.6 (0.5-0.6)**†
Angiogenesis			
HIF-1α	1 (0.8-1.2)	1.1 (0.9-1.1)	0.9 (0.8-1.6)
CD31	1 (0.5-1.5)	1.5 (1.4-1.6)	1.6 (1.3-1.8)
VEGF A	1 (1.0-1.0)	0.9 (0.8-0.9)	1.0 (0.7-1.1)
TSP-1	1 (0.7-1.5)	0.5 (0.4-0.7)	0.6 (0.6-1.6)
Smooth muscle cells			
α- SMA	1 (0.2-2.0)	1.1 (1.0-1.2)	0.7 (0.5-0.9)

Results are expressed as the median value (IQR) relative to the median value measured in PET 0 taken as 1. Mann-Whitney U test: *, $p<0.05$; **, $p<0.01$; ***, $p<0.001$ vs PET 0. Wilcoxon signed rank test: †, $p<0.05$; ††, $p<0.01$ vs negative site of PET +. nd, not detectable.

Supplemental Table 4. Relative expression of selected genes in the adventitia of AAA wall from PET0 and PET+ patients at the negative and positive site

Gene	PET0	PET+	
	(n=5)	Negative site (n=6)	Positive site (n=6)
Matrix remodeling			
MMP-1	1 (0.8-1.1)	1.8 (1.1-3.0)	22.9 (11.1-26.5)*
MMP-2	1 (0.9-1.2)	0.9 (0.8-1.0)	1.4 (1.2-1.7)*
MMP-3	1 (0.2-1.1)	0.6 (0.2-1.7)	0.7 (0.5-1.7)
MMP-9	1 (0.7-3.7)	2.0 (0.9-4.5)	4.5 (1.6-7.3)
MMP-12	nd	nd	nd
MMP-13[1]	nd	0.1 (0.0-0.1)	9.1 (1.5-20.0)
MMP-14	1 (0.9-1.0)	1.3 (1.0-1.9)	2.1 (1.8-2.3)**†
MMP-15	1 (0.9-1.4)	1.1 (1.0-1.1)	0.9 (0.8-1.0)
TIMP-1	1 (1.0-1.2)	1.1 (0.7-1.6)	1.3 (1.2-1.6)*
TIMP-2	1 (0.5-1.1)	0.8 (0.8-1.1)	0.7 (0.6-0.7)†
TIMP-3	1 (0.6-1.0)	0.8 (0.5-1.2)	1.0 (0.5-1.1)
PAI-1	1 (0.8-1.0)	1.0 (0.7-1.3)	1.8 (1.6-2.1)*
uPA	1 (0.7-1.1)	1.5 (0.8-2.2)	3.2 (1.8-3.3)*†
RECK	1 (0.9-1.0)	0.7 (0.7-0.9)	0.8 (0.7-0.8)*
EMMPRIN	1 (0.6-1.1)	0.9 (0.9-1.0)	0.7 (0.7-0.7)†
Structural proteins			
COL1A1	1 (0.8-1.1)	1.4 (1.0-2.6)	7.6 (5.8-9.5)**†
Elastin	1 (0.4-1.7)	1.2 (1.1-1.3)	1.1 (0.9-1.5)
Inflammatory mediators			
MCP-1	1 (0.7-1.0)	0.7 (0.5-1.1)	0.6 (0.5-0.9)
IL-1 β	1 (0.8-1.2)	1.5 (0.5-3.0)	1.0 (0.8-1.3)
IL-6	1 (0.9-1.0)	3.7 (0.8-5.3)	1.2 (0.4-4.0)

IL-8	1 (0.9-1.0)	2.5 (0.9-9.5)	1.5 (1.0-2.1)
COX-2	1 (0.9-1.3)	2.2 (0.8-4.2)	0.8 (0.5-1.2)
TNF-α	1 (0.7-1.8)	0.5 (0.4-0.7)*	0.5 (0.5-0.5)*
TGF-β	1 (0.9-1.0)	0.8 (0.7-0.9)*	0.7 (0.6-0.8)*
Angiogenesis			
HIF-1 α	1 (0.9-1.1)	1.1 (0.8-1.8)	1.5 (1.5-2.2)
CD31	1 (0.9-1.1)	0.9 (0.6-1.1)	0.8 (0.7-0.8)**
VEGF A	1 (1.0-1.5)	1.0 (0.7-1.5)	0.6 (0.6-0.8)*†
TSP-1	1 (0.8-3.5)	0.7 (0.3-1.0)	1.3 (0.4-2.6)†
Smooth muscle cells			
α- SMA	1 (0.8-1.9)	1.6 (1.2-2.3)	1.1 (0.6-1.5)

Results are expressed as the median value (IQR) relative to the median value measured in PET 0 taken as 1. Mann-Whitney U test: *, $p<0.05$; **, $p<0.01$; ***, $p<0.001$ vs PET 0. Wilcoxon signed rank test: †, $p<0.05$; ††, $p<0.01$ vs negative site of PET +. nd, not detectable. [1]MMP13 was not detected in PET0 samples and very weakly in negative site of PET+ samples, the median value in the positive site was calculated using the lowest value as 1.

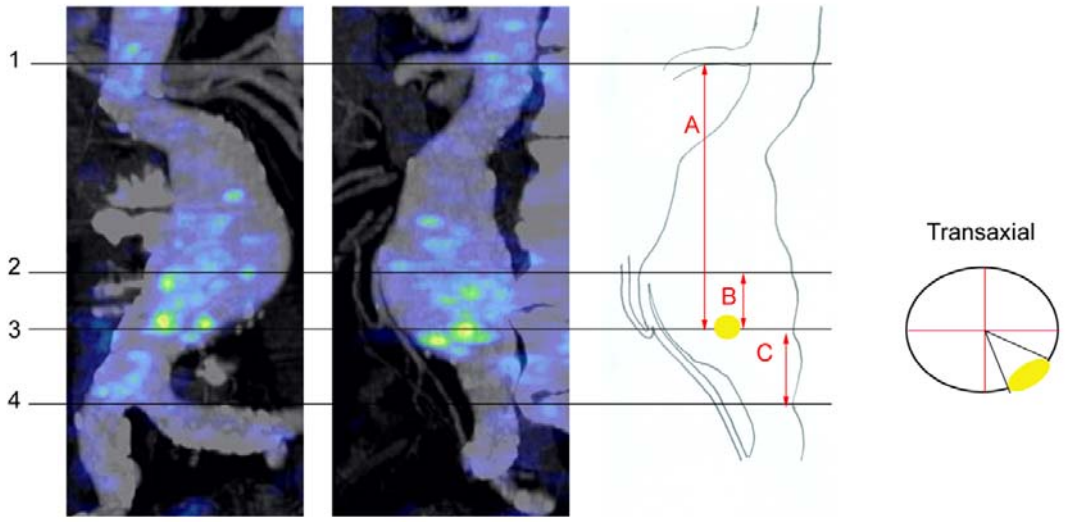

Supplemental Figure 1. Localisation of FDG uptake by anatomical landmarks. 1. Level of renal artery; 2. Level of inferior mesenteric artery; 3. Level of FDG uptake; 4. Level of bifurcation. The distances between the different levels and the positive spot were measured. A) distance between the renal artery and uptake; B) distance between inferior mesenteric artery and uptake and C) distance between uptake and bifurcation. These measurements are completed by measuring the distance between the positive spot and virtual axes on a transaxial image.

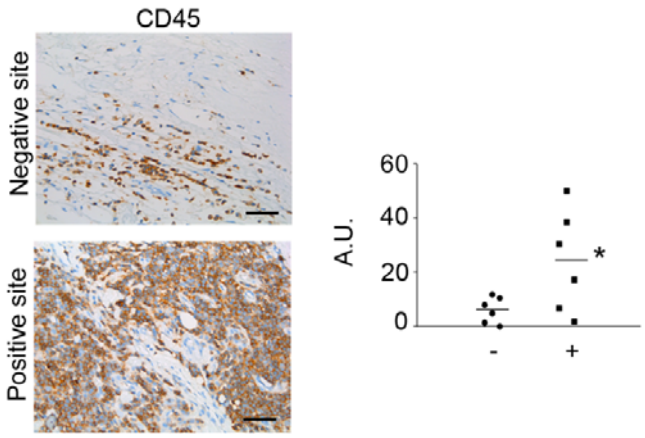

Supplemental Figure 2. Immunolabeling of generic leukocytes (CD45) in the negative and positive sites of FDG uptake from the same patient. Semi-quantification was performed in 6 pairs of samples. *, $p<0.05$, Wilcoxon signed rank test. Bar= 50µm.

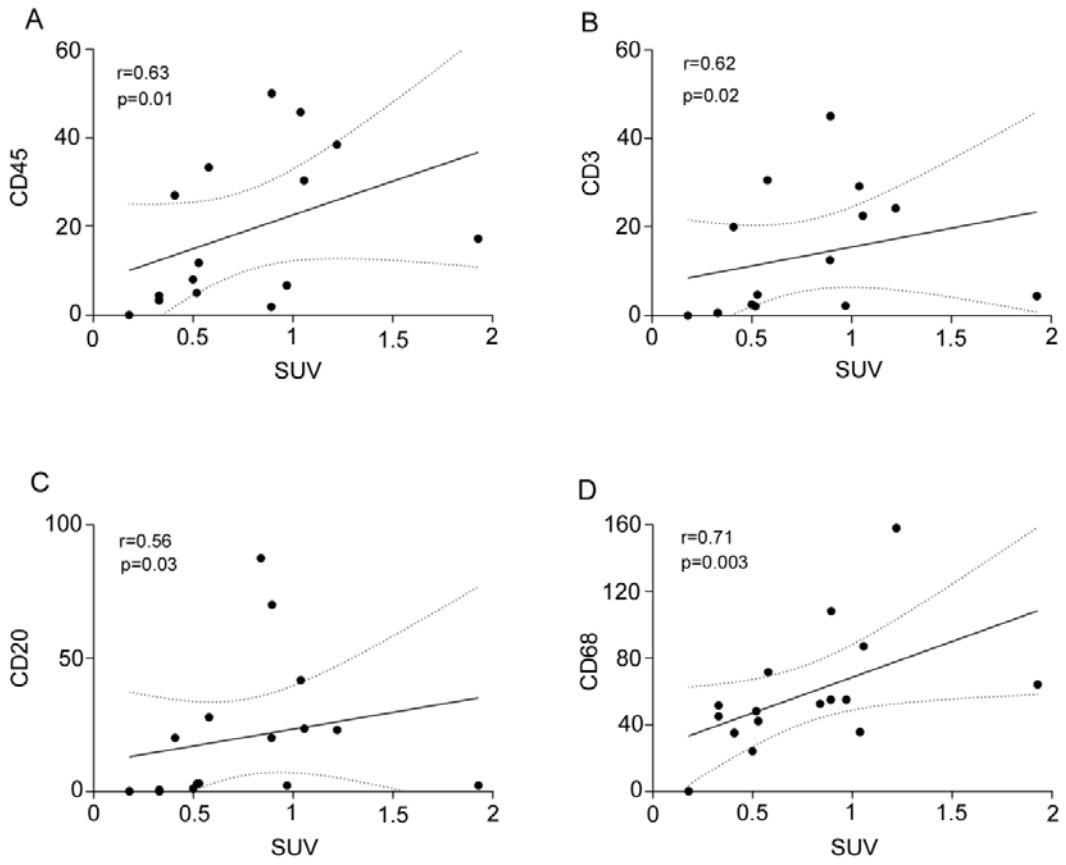

Supplemental Figure 3. Correlation between SUV and inflammatory cells density. Correlation between SUV and CD45- (A), CD3- (B), CD20- (C) and CD68-positive cells (D) was established with the Spearman's rank test. The regression curve and the 95% confidence intervals are shown (n=16).

.

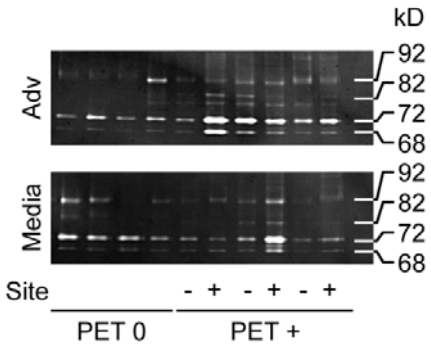

Supplemental Figure 4. MMP-2 and MMP-9 zymography of representative samples collected from the adventitia (Adv) and the media of PET0 patients and PET+ patients at the negative (minus) or at the positive site (plus). Pro-MMP9 (92 kDa), active MMP9 (82 kDa), pro-MMP2 (72 kDa) and active MMP2 (68 kDa) were observed.